

Spatial Correlation Unifies Nonequilibrium Response Theory for Arbitrary Markov Jump Processes

Jiming Zheng* and Zhiyue Lu†

Department of Chemistry, University of North Carolina-Chapel Hill, NC

(Dated: February 10, 2025)

Understanding how systems respond to external perturbations is a fundamental challenge in physics, particularly for non-equilibrium and non-stationary processes. The fluctuation-dissipation theorem provides a complete framework for near-equilibrium systems, and various bounds are recently reported for specific non-equilibrium regimes. Here, we present an exact response equality for arbitrary Markov processes that decompose system response into spatial correlations of local dynamical events. This decomposition reveals that response properties are encoded in correlations between transitions and dwelling times across the network, providing a natural generalization of the fluctuation-dissipation theorem to generic non-equilibrium processes. Our theory unifies existing response bounds, extends them to time-dependent processes, and reveals fundamental monotonicity properties of the tightness of multi-parameter response inequalities. Beyond its theoretical significance, this framework enables efficient numerical evaluation of response properties from sampling unperturbed trajectory, offering significant advantages over traditional finite-difference approaches for estimating response properties of complex networks and biological systems far from equilibrium.

Introduction.— The measurement and prediction of system response to external perturbations stands as a fundamental challenge in physics. The celebrated fluctuation-dissipation theorem (FDT) [1] revealed that near equilibrium, a system’s response to weak perturbations is fully determined by its equilibrium fluctuations. This principle is captured by the relation $\frac{\partial \langle Q \rangle}{\partial \lambda} = \beta \text{Cov}_{\text{eq}}(Q, \Lambda)$, showing that an observable Q ’s response to a parameter perturbation λ is encoded in its equilibrium correlation with the parameter’s conjugate variable Λ . This remarkable result demonstrates that a system’s response properties are accessible through equilibrium measurements alone, without the need for perturbative experiments.

Non-equilibrium systems, ubiquitous in nature and technology, present a broader challenge for response theory. Recent advances in the stochastic thermodynamics framework [2–7] allow us to classify non-equilibrium processes into the following three types.

The first type refers to processes maintained at/near non-equilibrium steady states (NESS), where the time-independent transition rates break detailed balance conditions. Yet, the system’s state probability reaches and maintains at the stationary distributions. Recently, studies on NESS response relations have established both inequalities [8–14] and equalities [11–15].

The second type refers to non-equilibrium relaxation processes (NERP), where a system evolves under a set of time-independent transition rates. Given sufficient time, these systems may eventually relax to either a NESS (for broken detailed balance) or equilibrium state (given detailed balance). Compared to NESS, such relaxation processes can exhibit complex phenomena such as adaptive responses in biological systems [16–18] and generalized Mpemba effects [19–24]. Very recently, responsiveness inequalities [25] and equalities [15] were introduced for

both perturbative and finite-perturbation response relations, establishing fundamental relations on system response away from NESS.

The third type refers to the most generic non-equilibrium processes (GNEP) where both the unperturbed dynamics and the perturbation could be time-dependent. Under the assumption that the unperturbed dynamics are time-homogeneous, a recent mathematical study established an equality for the time-dependent perturbation responses and discussed its Martingale property [26]. Under another assumption that the perturbation is time-independent, response equalities have been explored by Mase, Chatelain, and Ricci-Tersenghi [27–29]. For the most generic case of GNEP, only inequality relations have been reported [30, 31]. A generic non-equilibrium response theory for GNEP is still missing.

While previous approaches have established response relations for specific non-equilibrium regimes or under restrictive assumptions, this Letter presents a universal response equality applicable for Markov processes arbitrarily far from equilibrium (including equilibrium, NESS, NERP, and GNEP). The result reveals that the response of any observable to external perturbations is completely encoded in spatial correlations of local transition and dwelling events, providing a natural and informative extension of the equilibrium FDT to arbitrary non-equilibrium processes. The theory reveals both conceptual insights and computational advantages. Notably, this spatial decomposition enables a novel numerical approach to evaluating system response properties with significant speedup over traditional finite-difference methods.

Setup.—The dynamics of a n -state Markov jump process is governed by the master equation for the time evo-

lution of state probabilities

$$\frac{\partial \mathbf{p}(t)}{\partial t} = R \cdot \mathbf{p}(t), \quad (1)$$

where $\mathbf{p}(t) = (p_1(t), p_2(t), \dots, p_n(t))^\top$ is the column vector of probability distributions on the n states and $R = \{R_{ij}\}_{n \times n}$ is the transition rate matrix with diagonal elements $R_{ii} = \sum_{j, j \neq i} R_{ji}$.

For non-stationary processes, $\mathbf{p}(t)$ alone cannot fully capture the system dynamics. The probability distribution over stochastic trajectories provides a more complete description [32]. For discrete-state Markov processes, a stochastic trajectory X_τ can be denoted by a sequence of N jump events:

$$X_\tau = ((x_0, t_0), (x_1, t_1), \dots, (x_\alpha, t_\alpha), \dots, (x_N, t_N)), \quad (2)$$

where the system initiates at x_0 (at $t_0 = 0$) and undergoes a series of N transitions from state $x_{\alpha-1}$ to x_α at times t_α with $\alpha = 1, 2, \dots, N$. For any Markov process, the trajectory probability can be generally expressed by the products of the probabilities of jump events and probabilities of dwelling in between adjacent jumps:

$$\mathcal{P}[X_\tau] = p_{x_0}(t_0) \prod_{\alpha=1}^N R_{x_\alpha x_{\alpha-1}} \prod_{\alpha=0}^N e^{\int_{t_\alpha}^{t_{\alpha+1}} R_{x_\alpha x_\alpha} dt}, \quad (3)$$

where $t_{N+1} = \tau$ denote the ultimate time of the trajectory.

Any physical observable measured during the time τ can be generally denoted by a functional of stochastic trajectories $Q[X_\tau]$, and both Q and X_τ are stochastic variables. The expectation value of an observable from an ensemble of trajectories (obtained through repeated measurements) can be obtained by integrating over the trajectory probability density:

$$\langle Q \rangle = \int Q[X_\tau] \mathcal{P}[X_\tau] \mathcal{D}[X_\tau]. \quad (4)$$

From here, unless otherwise explained, the notation $\langle \cdot \rangle$ denotes path integral weighted by the trajectory probabilities. Here we denote the variance of observable Q by $\text{Var}[Q] = \langle Q^2 \rangle - \langle Q \rangle^2$.

In this Letter, we study generic non-equilibrium processes characterized by a transition rate matrix $R(t; \lambda)$ with arbitrary time dependence in both the unperturbed rates and perturbations. The control parameter could either represent external experimental conditions, such as temperature, external field, and chemical concentrations, or represent tunable internal kinetic parameters, such as the energy barrier between two states. Furthermore, when the external perturbation is time-dependent, the control parameter λ denotes the intensity of the time-dependent perturbation. For all scenarios, the generic non-equilibrium response sensitivity can be defined by a derivative: $\partial \langle Q \rangle / \partial \lambda$.

Universal response relations.—The response of any observable to external control can be determined from understanding how trajectory probabilities change with the control parameter λ . This change is characterized by

$$\frac{\partial \mathcal{P}[X_\tau; \lambda]}{\partial \lambda} = \Lambda[X_\tau; \lambda] \mathcal{P}[X_\tau; \lambda]. \quad (5)$$

Here we denote the control parameter's conjugate $\Lambda[X_\tau, \lambda]$ as the score function that is defined by $\Lambda \equiv \partial \ln \mathcal{P}[X_\tau; \lambda] / \partial \lambda$.

Due to the normalization of trajectory probabilities, the expectation value of Λ must always be zero. Using this property, Eqs. (4) and (5), and the chain rule, a general response relation for any trajectory observable $\langle Q \rangle$ can be written as:

$$\frac{\partial \langle Q \rangle}{\partial \lambda} = \left\langle \frac{\partial Q}{\partial \lambda} \right\rangle + \text{Cov}(Q, \Lambda), \quad (6)$$

where the covariance function $\text{Cov}(Q, \Lambda) \equiv \langle Q\Lambda \rangle - \langle Q \rangle \langle \Lambda \rangle = \langle Q\Lambda \rangle$ since $\langle \Lambda \rangle = 0$. Additionally, the first term of the r.h.s. can be ignored if the observable $Q[X_\tau]$ does not explicitly depend on the control parameter. The above relation is true for all types of non-equilibrium processes.

It appears challenging to utilize the above response equality due to the difficulties in obtaining the score function Λ for arbitrarily controlled systems and various choices of λ . However, this Letter demonstrates that, via spatial-temporal decomposition of the dynamics, the response can be described by the combination of the covariance between Q and edge-wise local observables $\{\Theta_{ij}\}$.

For NERP, where the non-equilibrium relaxation is governed by a time-independent rate matrix $R(\lambda)$. By choosing $\lambda = \ln R_{ij}$, the conjugate variable Λ becomes the *dynamical discrepancy*,

$$\Theta_{ij}[X_\tau] \equiv N_{ij}[X_\tau] - R_{ij} T_j[X_\tau] \quad (7)$$

which is a fundamental quantity of our response theory. Here, $N_{ij}[X_\tau]$ is the total number of transitions from state j to state i , and $T_j[X_\tau]$ is the total dwelling time on state j , both evaluated from a realization of the trajectory X_τ . Averaged over an ensemble of trajectories, the expectation values of N_{ij} and $R_{ij} T_j$ must equal each other for an arbitrary Markov process, and thus $\langle \Theta_{ij} \rangle = 0$. For each realization of the stochastic process X_τ , the dynamical discrepancy $\Theta_{ij}[X_\tau]$ quantifies the stochastic mismatch between the number of jumps N_{ij} and the transition-rate-weighted dwelling time $R_{ij} T_j$ that is obtained by one realization (i.e., one trajectory X_τ). The dynamical discrepancies on all transition edges $\{\Theta_{ij}\}$ offers a spatial decomposition of Λ :

$$\Lambda[X_\tau] = \sum_{i \neq j} \frac{\partial \ln R_{ij}}{\partial \lambda} \Theta_{ij}. \quad (8)$$

Therefore, the response of any trajectory observable $\langle Q \rangle$ can be decomposed into contributions from each transition edge:

$$\frac{\partial \langle Q \rangle}{\partial \lambda} = \left\langle \frac{\partial Q}{\partial \lambda} \right\rangle + \sum_{i \neq j} \frac{\partial \ln R_{ij}}{\partial \lambda} \text{Cov}(Q, \Theta_{ij}). \quad (9)$$

The above decomposition implies that a system's non-equilibrium response could be obtained by a weighted summation over correlations between the observable and the dynamical discrepancy on each transition edge. It provides both theoretical insights and numerical advantages in understanding and computing non-equilibrium system's responses to external perturbations. Notice that the above results, Eqs. (7) to (9), generally hold for any time-inhomogeneous Markovian jump dynamics. Thus, it applies to both NESS and NERP processes.

For time-dependent transition rates $R_{ij}|_{\lambda=0}$ and/or time-dependent perturbations $\left. \frac{\partial \ln R_{ij}}{\partial \lambda} \right|_{\lambda=0}$, i.e., general non-equilibrium processes (GNP), we can obtain a similar temporal-spatial decomposition of the response relation. Here, for each transition edge, we define the dynamical discrepancy accumulation rate

$$\dot{\Theta}_{ij}[X_\tau] = \dot{N}_{ij}(t) - R_{ij}(t)\delta_{x(t),j} \quad (10)$$

where $N_{ij}(t)$ is the accumulated transitions from j to i within time $[0, t)$ for a realization X_τ , and $\delta_{x(t),j}$ is a Kronecker delta that equals unity when the system state is $x(t) = j$. Under this decomposition, the control-conjugate variable within the general non-equilibrium response relation (Eq. (6)) can be represented by the following spatial-temporal decomposition:

$$\Lambda[X_\tau] = \sum_{i \neq j} \int_0^\tau \frac{\partial \ln R_{ij}(t)}{\partial \lambda} \dot{\Theta}_{ij}[X_\tau] dt. \quad (11)$$

If both $R_{ij}|_{\lambda=0}$ and $\left. \frac{\partial \ln R_{ij}}{\partial \lambda} \right|_{\lambda=0}$ are time-independent, Eq. (11) reduces to Eq. (8).

Spatial correlation analysis.—The above analysis indicates that the dynamical discrepancy $\{\Theta_{ij}\}$ is a key stochastic quantity that encodes the system information on each edge. It also has good statistical properties. Firstly, its zero-mean property is a consequence of $\langle N_{ij} \rangle = R_{ij} \langle T_j \rangle$. Secondly, the spatial correlations of $\{\Theta_{ij}\}$ between any pair of transition edges are:

$$\text{Cov}(\Theta_{ij}, \Theta_{kl}) = \langle N_{ij} \rangle \delta_{(i,j),(k,l)}, \quad (12)$$

where $\delta_{(i,j),(k,l)}$ is the Kronecker delta as defined below:

$$\delta_{(i,j),(k,l)} = \begin{cases} 1, & i = k \text{ and } j = l, \\ 0, & \text{else.} \end{cases} \quad (13)$$

This result indicates that the variance of dynamical discrepancy for an edge characterizes its average transition

frequency. Furthermore, it reveals that the dynamical discrepancies of two arbitrary edges are statistically uncorrelated. It confirms that $\{\Theta_{ij}\}$ forms a suitable basis for describing a system's response properties. Eq. (12) can be proven by taking derivatives twice on both sides of the trajectory probability in Eq. (3).

The above analysis covers the spatial decomposition of the conjugate variable Λ into dynamical discrepancies for each edge. In the following, we further state that the decomposition of observables Q implies that spatial correlations determine their non-equilibrium response properties.

Physical observables of a Markov system can usually be decomposed into "local contributions". In general, one can construct an observable by combining two observable types: counting and dwelling. For example, current and traffic [33] are transition-counting observables and state average observables are state-dwelling observables. Thus, for a general observable, we can usually decompose it as

$$Q[X_\tau] = \sum_{i \neq j} a_{ij}(\lambda) \cdot N_{ij}[X_\tau] + \sum_k b_k(\lambda) \cdot T_k[X_\tau], \quad (14)$$

where a_{ij} is the accumulation weight associated with each transition event and b_k is the weight associated with dwelling at state k . With the decompositions of Q and Λ , one can conclude that, for any observable, the response can always be decomposed into the linear combination of spatial correlations $\text{Cov}(N_{ij}, N_{kl})$, $\text{Cov}(N_{ij}, T_k)$, and $\text{Cov}(T_i, T_j)$ on different edges or states. Moreover, if all the coefficients $\{a_{ij}, b_k\}$ are independent of the parameter λ , the first term on the right-hand side of Eq. (6) vanishes. In this scenario, the response of any non-equilibrium process in terms of any arbitrary observable is entirely encoded by the spatial correlations of the dynamics from the unperturbed process (i.e., transitions and dwells), which are easy to obtain.

A particularly insightful result emerges when we consider spatially localized quantities. When both the observable Q and the perturbation λ are confined to specific edges of the network, our theory reveals an interesting property: the response depends only on the correlation between these edges, regardless of their separation in the network. For instance, by choosing $Q = a_{ij} N_{ij}$ and $\lambda = \ln R_{kl}$, where the edges (ij) and (kl) are arbitrarily far apart, the response $\partial \langle Q \rangle / \partial (\ln R_{kl}) = a_{ij} \text{Cov}(N_{ij}, \Theta_{kl})$ is fully determined by the statistical correlation between the two edges of interest, $i \leftarrow j$ and $k \leftarrow l$, yet no explicit information about other edges of the graph is involved.

Numerical Applications—Our response equality leads to a novel numerical approach, significantly reducing the sampling cost for computing system responses. Traditional estimation of the system's responses toward external control parameters typically involves finite difference methods that suffer from an inherent accuracy-cost trade-off. Furthermore, the numerical effort for estimating a response gradient of multi-dimensional control

$\lambda = (\lambda_1, \lambda_2, \dots, \lambda_{N_{\text{para}}})$ scales with the number of parameters. Our approach allows us to efficiently estimate multi-variable response properties from numerically sampling trajectories from a single unperturbed simulation.

When estimating a system's response to a given control parameter λ , the traditional finite difference method estimates responses by performing two sets of simulations and comparing the differences:

$$\frac{\partial \langle Q \rangle}{\partial \lambda} \approx \eta \equiv \frac{\langle Q \rangle_{\text{ptb}} - \langle Q \rangle_{\text{unptb}}}{\Delta \lambda}. \quad (15)$$

where the expectation $\langle Q \rangle$ is estimated from an ensemble of N_{traj} independent stochastic trajectories which can be obtained by repeated kinetic Monte Carlo simulations:

$$\langle Q \rangle \approx \bar{Q} \equiv \frac{1}{N_{\text{traj}}} \sum_{i=1}^{N_{\text{traj}}} Q[X_\tau^{(i)}], \quad (16)$$

where $X_\tau^{(i)}$ stands for the i -th sampled trajectory.

Firstly, the finite difference approach suffers from *accuracy-precision-cost trade-off*: On the one hand, unless the response is strictly linear, the estimated response sensitivity carries a systematic error for any finite $\Delta \lambda$, creating a trade-off between accuracy and precision at a given computational cost. On the other hand, there is a tradeoff between the precision and the computational cost: Since the difference in observable decays with $\Delta \lambda$, resulting in the need for a larger sampling size N_{traj} . According to the law of large numbers, $\bar{Q} \rightarrow \mathcal{N}(\mu(Q), \frac{\sigma^2(Q)}{N_{\text{traj}}})$ as $N_{\text{traj}} \rightarrow +\infty$ with μ and σ representing expectation and standard deviation, respectively. The finite-difference resolution between the perturbed and unperturbed observables can be captured by the signal-to-noise ratio:

$$\text{SNR} \equiv \frac{|\mu_{\text{ptb}}(\bar{Q}) - \mu_{\text{unptb}}(\bar{Q})|}{\sqrt{\frac{\sigma_{\text{ptb}}^2(\bar{Q}) + \sigma_{\text{unptb}}^2(\bar{Q})}{2}}} \quad (17a)$$

$$\approx \frac{|\eta \Delta \lambda| \cdot \sqrt{2N_{\text{traj}}}}{\sqrt{\text{Var}_{\text{ptb}}[Q] + \text{Var}_{\text{unptb}}[Q]}}. \quad (17b)$$

This analysis illustrated the precision-cost trade-off relation that the required sampling size scales with $N_{\text{traj}} \propto \frac{1}{\Delta \lambda^2}$. Therefore, to achieve higher accuracy (low systematic error), one needs a smaller $\Delta \lambda$, which results in a larger sampled trajectory number to maintain the same resolution.

Secondly, traditional finite difference requires a large number of simulations for estimating the sensitivity gradient of a high-dimensional control parameter vector λ . In this case, the same finite difference procedure needs to be repeated N_{para} times to obtain the response properties for all parameters.

In contrast, our response equality Eq. (6) avoids both difficulties by converting the sensitivity estimation problem into an estimation of spatial correlations:

$\text{Cov}(N_{ij}, N_{kl})$, $\text{Cov}(N_{ij}, T_k)$, and $\text{Cov}(T_i, T_j)$. This correlation estimation does not suffer from the accuracy-sampling trade-off difficulty illustrated above, and it only requires one set of simulations (on the unperturbed system) to obtain all partial derivatives within the sensitivity gradient. A numerical comparison of our approach and traditional finite difference approach is shown in the *End Matter*.

Unification of Response Uncertainty Relations.—Our non-equilibrium response theory advances the understanding of existing response inequalities in three fundamental ways. First, by expressing Fisher information through edge-wise contributions, our theory extends Response Uncertainty Relations (RUR) to all generic types of non-equilibrium processes. Second, the spatial decomposition described in this Letter reveals deep connections to the high-dimensional Cramér-Rao bounds with multi-dimension observables and parameters. Third, we discover fundamental information monotonicity properties of the responsiveness inequality tightness under different choices of control parameters.

The theory proposed in this Letter connects to existing inequalities [9–12], known as RUR, via Fisher information while generalizing them from NESS to GNEP. In any generic non-equilibrium process, the Fisher information $\mathcal{I}(\lambda) = \text{Var}[\Lambda]$ equals the variance of the score function Λ , which we obtain by taking the ensemble average of the derivative of Eq. (5):

$$\mathcal{I}(\lambda) = \text{Var}[\Lambda] = - \left\langle \frac{\partial \Lambda}{\partial \lambda} \right\rangle \quad (18a)$$

$$= \left\langle \sum_{i \neq j} \int_0^\tau \left(\frac{\partial \ln R_{ij}(t)}{\partial \lambda} \right)^2 R_{ij} \delta_{x(t),j} dt \right\rangle, \quad (18b)$$

This formulation reveals how Fisher information decomposes into contributions from local dynamical events across the network. For processes with a time-independent rate matrix, such as NESS and NERP, the Fisher information is reduced to a linear combination of averaged transitions $\mathcal{I}(\lambda) = \sum_{i \neq j} \left(\frac{\partial \ln R_{ij}}{\partial \lambda} \right)^2 \langle N_{ij} \rangle$. By choosing $\lambda = R_{ij}$, it reduces to the result in [25]: $\mathcal{I} = \langle N_{ij} \rangle / R_{ij}^2$. Furthermore, our theory refines the result in [31] with Fisher information $\mathcal{I}(\lambda) = \langle Z_{ij}^2 R_{ij} T_j \rangle$ given the transition rates following $R_{ij} = k_{ij} e^{\lambda Z_{ij}}$.

With this expression for Fisher information, the Fluctuation-Response Inequality (FRI) for NERP [31] can be obtained from our general response relation through the Cauchy-Schwarz inequality:

$$\frac{\left(\frac{\partial \langle Q \rangle}{\partial \lambda} - \left\langle \frac{\partial Q}{\partial \lambda} \right\rangle \right)^2}{\text{Var}[Q]} \leq \text{Var}[\Lambda] = \mathcal{I}(\lambda). \quad (19)$$

Furthermore, our theory indicates that the FRI bounds saturate if and only if the observable Q and the score

function Λ are linearly dependent:

$$Q \propto \Lambda = \sum_{i \neq j} \frac{\partial \ln R_{ij}}{\partial \lambda} N_{ij} + \sum_k R_{kk} \frac{\partial \ln R_{kk}}{\partial \lambda} T_j. \quad (20)$$

Our framework reveals a rich structure for processes with multi-dimensional observables or control parameters through high-dimension Cramér-Rao inequalities. There are two types of multi-dimensional Cramér-Rao inequalities:

- (1) The first type addresses multiple observables. For K observables $\mathbf{Q}^{(K)} = (Q_1, \dots, Q_K)$, one obtains

$$(\partial_\lambda \langle \mathbf{Q}^{(K)} \rangle)^\top (\Xi_Q^{(K)})^{-1} (\partial_\lambda \langle \mathbf{Q}^{(K)} \rangle) \leq \mathcal{I}(\lambda), \quad (21)$$

where $(\Xi_Q^{(K)})_{ij} = \text{Cov}(Q_i, Q_j)$ is the covariance matrix of $\mathbf{Q}^{(K)}$. This result leads to multi-dimensional Thermodynamic Uncertainty Relations (TUR) and FRI as reported in [34, 35].

- (2) The second type involves multiple parameters $\boldsymbol{\lambda} \in \mathbb{R}^K$, yielding:

$$\Psi^\lambda \equiv (\partial_\lambda \langle Q \rangle)^\top (\mathcal{I}(\boldsymbol{\lambda}))^{-1} (\partial_\lambda \langle Q \rangle) \leq \text{Var}[Q], \quad (22)$$

where $\partial_\lambda \langle Q \rangle = (\partial_{\lambda_1} \langle Q \rangle, \dots, \partial_{\lambda_K} \langle Q \rangle)$ and the entries of Fisher information matrix is $(\mathcal{I}(\boldsymbol{\lambda}))_{ij} = -\langle \partial_{\lambda_i} \partial_{\lambda_j} \ln \mathcal{P}[X_T] \rangle$. Recent work [9] reported that the multi-parameter inequality leads to RUR and the recent conjectured R-TUR [10].

When the observable Q is λ -dependent, the $(\partial_\lambda \langle Q \rangle)$ should be replaced by $(\partial_\lambda \langle Q \rangle - \langle \partial_\lambda Q \rangle)$ for the above inequalities. Interestingly, we can prove that the two types of multi-dimensional Cramér-Rao inequalities are equivalent when we choose dynamical discrepancies as observables $Q_\alpha = \Lambda_\alpha$ for all $2 \leq \alpha \leq K$. Detailed derivations are discussed in the supplementary material.

The spatial correlations of $\{\Theta_{ij}\}$ in Eq. (12) implies that the multi-parameter Fisher information matrix is diagonal if and only if each parameter only affects one local edge. Consider a more general scenario, where each parameter λ_α affects n_α edges $\mathbf{e}^{(\alpha)} = (e_1^{(\alpha)}, e_2^{(\alpha)}, \dots, e_{n_\alpha}^{(\alpha)})$, where $\alpha \in (1, 2, \dots, K)$. If the controls are mutually exclusive: $\mathbf{e}^{(\alpha)} \cap \mathbf{e}^{(\alpha')} = \emptyset$ for any α and α' , then the multi-parameter Fisher information becomes diagonal, significantly simplifying the bounds.

Our analysis of the Cramér-Rao inequality applies to both NESS and GNEP. Here, we find out that the RUR for generic non-equilibrium processes assumes the same form as the previously reported RUR for NESS [9]. To illustrate this, consider localized control parameters as edge kinetic barrier $B_{ij} = B_{ji}$ or edge force $F_{ij} = -F_{ji}$ from the rate formula

$$R_{ij} = e^{B_{ij} + F_{ij}/2}, \quad (23)$$

where each parameter only affects a single edge. In this case, our inequality extends the following two sets of RURs

$$\sum_{i \leq j} \frac{(\partial_{B_{ij}} \langle Q \rangle)^2}{\langle N_{ij} \rangle} \leq \text{Var}[Q], \quad \sum_{i \leq j} \frac{4(\partial_{F_{ij}} \langle Q \rangle)^2}{\langle N_{ij} \rangle} \leq \text{Var}[Q], \quad (24)$$

from NESS [9] to arbitrary time-dependent processes.

Ultimately, these multi-dimension Cramér-Rao analyses reveal two fundamental monotonicity properties that characterize the information content of response inequalities. First, adding extra parameters leads to tighter bounds. The information monotonicity states that $\Psi^\lambda \leq \Psi^{\lambda, \lambda'}$. The inequality saturates if and only if the newly added parameter linearly depends on the old ones. The proof of the inequality is similar to the one in [31]. Second, separating a global perturbation into independent local ones leads to tighter bounds. For a global parameter λ^* that affects $\mathbf{e}^{(*)}$ edges, its effect can be represented by some local parameters as $\lambda^* = \sum_\alpha \frac{\partial \lambda^*}{\partial \lambda_\alpha} \lambda_\alpha$ with $\mathbf{e}^{(\alpha)} \cap \mathbf{e}^{(\alpha')} = \emptyset$ and $\bigcup_\alpha \mathbf{e}^{(\alpha)} = \mathbf{e}^{(*)}$. In this case, the information monotonicity reads

$$\frac{(\partial_{\lambda^*} \langle Q \rangle)^2}{\text{Var}[\Lambda^*]} \leq \sum_\alpha \frac{(\partial_{\lambda_\alpha} \langle Q \rangle)^2}{\text{Var}[\Lambda_\alpha]} \leq \text{Var}[Q]. \quad (25)$$

Conclusion—This work establishes an exact universal response theory for Markov processes through the spatial decomposition of dynamical events. The theory naturally extends the fluctuation-dissipation theorem to arbitrary non-equilibrium and non-stationary processes, revealing that response properties are encoded in spatial correlations between transitions and dwelling times. This decomposition enables efficient numerical evaluation of response properties from unperturbed trajectory data, offering significant computational advantages over traditional methods. The framework unifies existing response bounds and further reveals fundamental monotonicity principles regarding the information encoded in multiple degrees of freedom of control parameters. These advances provide theoretical insights and practical tools for studying complex networks and biological systems arbitrarily far from equilibrium.

Acknowledgements—This work is supported by the National Science Foundation under Grant No. DMR-2145256.

* jiming@unc.edu

† zhiyuelu@unc.edu

[1] R. Kubo, Statistical-mechanical theory of irreversible processes. i. general theory and simple applications to magnetic and conduction problems, Journal of the physical society of Japan **12**, 570 (1957).

- [2] U. Seifert, Stochastic thermodynamics: principles and perspectives, *The European Physical Journal B* **64**, 423 (2008).
- [3] L. Peliti and S. Pigolotti, *Stochastic thermodynamics: an introduction* (Princeton University Press, 2021).
- [4] C. Van den Broeck, Stochastic thermodynamics: A brief introduction, in *Physics of Complex Colloids* (IOS Press, 2013) pp. 155–193.
- [5] J. Kurchan, Six out of equilibrium lectures, arXiv preprint arXiv:0901.1271 (2009).
- [6] R. Klages, W. Just, C. Jarzynski, and H. Schuster, *Nonequilibrium Statistical Physics of Small Systems: Fluctuation Relations and Beyond*, *Reviews of Nonlinear Dynamics and Complexity* (Wiley, 2013).
- [7] U. Seifert, Stochastic thermodynamics, fluctuation theorems and molecular machines, *Reports on progress in physics* **75**, 126001 (2012).
- [8] J. A. Owen, T. R. Gingrich, and J. M. Horowitz, Universal thermodynamic bounds on nonequilibrium response with biochemical applications, *Physical Review X* **10**, 011066 (2020).
- [9] E. Kwon, H.-M. Chun, H. Park, and J. S. Lee, Fluctuation-response inequalities for kinetic and entropic perturbations, arXiv preprint arXiv:2411.18108 (2024).
- [10] K. Ptasiński, T. Aslyamov, and M. Esposito, Dissipation bounds precision of current response to kinetic perturbations, *Physical Review Letters* **133**, 227101 (2024).
- [11] T. Aslyamov, K. Ptasiński, and M. Esposito, Nonequilibrium fluctuation-response relations: From identities to bounds, arXiv preprint arXiv:2410.17140 (2024).
- [12] K. Ptasiński, T. Aslyamov, and M. Esposito, Nonequilibrium fluctuation-response relations for state observables (2024), arXiv:2412.10233 [cond-mat.stat-mech].
- [13] T. Aslyamov and M. Esposito, General theory of static response for markov jump processes, *Physical Review Letters* **133**, 107103 (2024).
- [14] R. Bao and S. Liang, Nonequilibrium response theory: From precision limits to strong perturbation (2024), arXiv:2412.19602 [cond-mat.stat-mech].
- [15] P. E. Harunari, S. Dal Cengio, V. Lecomte, and M. Poletini, Mutual linearity of nonequilibrium network currents, *Physical Review Letters* **133**, 047401 (2024).
- [16] B. Wark, B. N. Lundstrom, and A. Fairhall, Sensory adaptation, *Current opinion in neurobiology* **17**, 423 (2007).
- [17] G. Lan, P. Sartori, S. Neumann, V. Sourjik, and Y. Tu, The energy–speed–accuracy trade-off in sensory adaptation, *Nature physics* **8**, 422 (2012).
- [18] D. Conti and T. Mora, Nonequilibrium dynamics of adaptation in sensory systems, *Physical Review E* **106**, 054404 (2022).
- [19] Z. Lu and O. Raz, Nonequilibrium thermodynamics of the markovian mpemba effect and its inverse, *Proceedings of the National Academy of Sciences* **114**, 5083 (2017).
- [20] I. Klich, O. Raz, O. Hirschberg, and M. Vucelja, Mpemba index and anomalous relaxation, *Physical Review X* **9**, 021060 (2019).
- [21] Z. Cao, R. Bao, J. Zheng, and Z. Hou, Fast functionalization with high performance in the autonomous information engine, *The Journal of Physical Chemistry Letters* **14**, 66 (2022).
- [22] S. S. Chittari and Z. Lu, Geometric approach to nonequilibrium hasty shortcuts, *The Journal of Chemical Physics* **159** (2023).
- [23] A. Pagare and Z. Lu, Mpemba-like sensory withdrawal effect, *PRX Life* **2**, 043019 (2024).
- [24] I. G.-A. Pemartín, E. Mompó, A. Lasanta, V. Martín-Mayor, and J. Salas, Shortcuts of freely relaxing systems using equilibrium physical observables, *Physical Review Letters* **132**, 117102 (2024).
- [25] J. Zheng and Z. Lu, Universal non-equilibrium response theory beyond steady states (2024), arXiv:2403.10952 [cond-mat.stat-mech].
- [26] A. Faggionato and V. Silvestri, A martingale approach to time-dependent and time-periodic linear response in markov jump processes, *ALEA Lat. Am. J. Probab. Math. Stat.* **21**, 863 (2024).
- [27] M. Baiesi, C. Maes, and B. Wynants, Fluctuations and response of nonequilibrium states, *Physical review letters* **103**, 010602 (2009).
- [28] C. Chatelain, A far-from-equilibrium fluctuation–dissipation relation for an ising–glauber-like model, *Journal of Physics A: Mathematical and General* **36**, 10739 (2003).
- [29] F. Ricci-Tersenghi, Measuring the fluctuation-dissipation ratio in glassy systems with no perturbing field, *Physical Review E* **68**, 065104 (2003).
- [30] K. Liu and J. Gu, Dynamical activity universally bounds precision of response, arXiv preprint arXiv:2410.20800 (2024).
- [31] A. Dechant and S.-i. Sasa, Fluctuation–response inequality out of equilibrium, *Proceedings of the National Academy of Sciences* **117**, 6430 (2020).
- [32] A. Pagare, Z. Zhang, J. Zheng, and Z. Lu, Stochastic distinguishability of markovian trajectories, *The Journal of Chemical Physics* **160** (2024).
- [33] C. Maes, Frenesy: Time-symmetric dynamical activity in nonequilibria, *Physics Reports* **850**, 1 (2020).
- [34] A. Dechant, Multidimensional thermodynamic uncertainty relations, *Journal of Physics A: Mathematical and Theoretical* **52**, 035001 (2018).
- [35] A. Dechant and S.-i. Sasa, Improving thermodynamic bounds using correlations, *Physical Review X* **11**, 041061 (2021).

End Matter

Numerical advantages.—Our universal response equality Eq. (6) together with the dynamical discrepancy Eqs. (7) and (10) significantly reduces the computational cost for response properties.

We first demonstrate the numerical advantages of our method over the finite difference method on a three-state Markov system. Consider the following unperturbed rate matrix

$$R = \begin{pmatrix} -130 & 30 & 70 \\ 90 & -40 & 50 \\ 40 & 10 & -120 \end{pmatrix}. \quad (26)$$

with the system initially prepared at state 1. We define the observable as the accumulated number of transitions from state 1 to 0. To estimate the response of $\langle N_{01} \rangle$ to

the control $\lambda = R_{21}$, we compare our method with the finite difference method, as shown in Fig. 1.

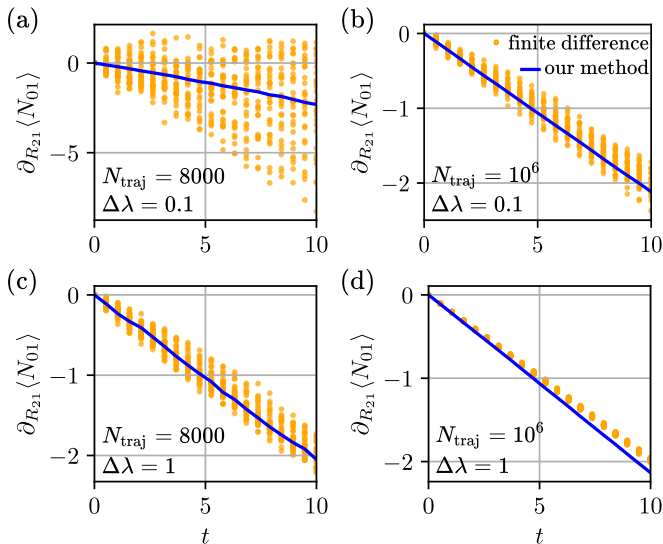


Figure 1. Four sets of kinetic Monte Carlo simulations on a three-state Markov system with the rate matrix in Eq. (26). Each point and curve is obtained from trajectory averages. The traditional finite difference method is repeated 30 times for each subfigure to show its convergence issue. The number of trajectories N_{traj} is 8000 for (a) and (c), and is 10^6 for (b) and (d). The $\Delta\lambda$ in finite difference method is 0.1 for (a) and (b), and is 1 for (c) and (d).

The main text mentions that the traditional finite difference method suffers from an accuracy-precision-cost trade-off relation. This issue is clearly illustrated by the numerical results represented by the orange dots in Fig. 1. Comparing Fig. 1(a) with (b) (or (c) with (d)), it shows that the larger the sampling size, the higher the precision (less spread of orange dots). The deviation between the orange dots and the blue curve (our method) in Fig. 1(d) shows that a finite $\Delta\lambda$ leads to a systematic error. Smaller $\Delta\lambda$ may improve this issue, but it immediately gives rise to a convergence issue as shown by comparing Fig. 1(b) with (d) (or (a) with (c)). In contrast, our method is free of this trade-off issue. The four blue curves in Fig. 1 show a consistent trend, representing the high accuracy, high precision, and low cost of our method. Also, by comparing our result with the fi-

nite difference result shown in Fig. 1(b), it indicates that the precision of the finite difference method is worse than ours even when we choose a relatively large sample size. Fig. 1(d) indicates that the systematic error of the finite difference method is more prominent for the large finite $\Delta\lambda$.

In the following example, we numerically illustrate that the advantage of our method is more prominent in larger networks. Here, we randomly generate a Markov graph with 100 states, as shown in Fig. 2(a). Starting from a non-stationary initial probability distribution, the system evolves toward the steady state corresponding to the rate matrix of the graph. In Fig. 2(b), we compare the sensitivity results from traditional finite difference approaches (orange dots) with results from our method (blue curves) under the same sampling size. By repeating the simulations for 15 times, our results indicate that our method captures the system's sensitivity well, yet the traditional finite difference method suffers from both low precision (extremely large variance) and low accuracy (positive systematic error).

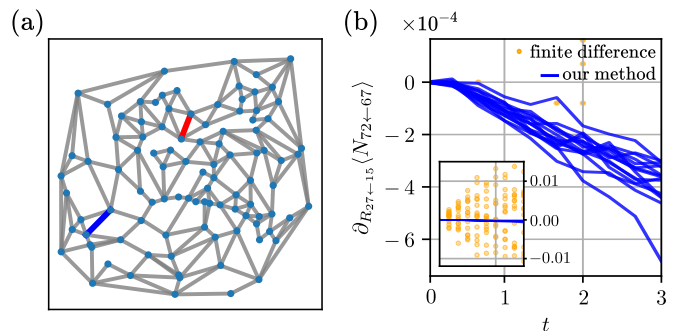


Figure 2. A Markov network graph with 100 states, with its transition rates randomly generated with values between 10 and 100. This system's kinetic Monte Carlo simulations are performed with the same initial probability (randomly generated). (a) The input edge (control) is in red, and the output edge (observable) is in blue. (b) In each realization, we perform the finite difference method (orange dots) and our method (blue curves) for the sampling size $N_{\text{traj}} = 2 \times 10^5$. We repeat these realizations 15 times to illustrate the variances. The parameter difference for the traditional finite difference method is $\Delta\lambda = 1$.